Materials Sciences and Applications, **2011, 2, 390-398**
doi:10.4236/msa.2011.25050 Published Online May 2011 (http://www.SciRP.org/journal/msa)

Elevated Temperatures Tensile Characteristics of Cast A356/Al_2O_3 Nanocomposites Fabricated Using a Combination of Rheocasting and Squeeze Casting Techniques

El-Sayed Youssef El-Kady, Tamer Samir Mahmoud, Mohamed Abdel-Aziz Sayed

Mechanical Engineering Department, Faculty of Engineering, King Khalid University (KKU), Abha, Kingdom of Saudi Arabia.
Email: Eyelkady@yahoo.com

Received December 24th, 2010; revised March 21st, 2011; accepted April 6th, 2011.

ABSTRACT

In the present investigation, the tensile properties of A356/Al_2O_3 nanocomposites at both ambient and elevated temperatures were studied. The A356/Al_2O_3 nanocomposites were fabricated using a combination between the rheocasting and squeeze casting techniques. The A356 matrix alloy was reinforced with Al_2O_3 nanoparticulates having average sizes of 60 nm and 200 nm with different volume fractions up to 5 vol%. The results revealed that the A356/Al_2O_3 nanocomposites exhibited better mechanical properties than the A356 monolithic alloy. Such improvement in the mechanical properties was observed at both room and elevated temperatures up to 300˚C. Increasing the volume fraction and/or reducing the size of Al_2O_3 nanoparticulates increase both the tensile and yield strengths of the nanocomposites.

Keywords: *Nanocomposites*, *Mechanical Properties*, *Rhecocasting*, *Squeeze Casting*, *Aluminum Alloys*

1. Introduction

Metal matrix composites (MMCs) exhibit attractive physical and mechanical properties such as high tensile, creep and fatigue strengths, superior wear resistance, and improved thermal stability. Such properties allow these materials to have numerous applications in the aerospace, automobile and military industries [1,2]. Normally, micro-size ceramic particles are used to improve the yield and ultimate strength of the metal. However, the ductility of the MMCs deteriorates with high ceramic particle concentration [3-5]. Recently, it is of interest to use nano-size ceramic particles to strengthen the metal matrix, while maintaining good ductility [6-8]. With nanoparticles reinforcement, high temperature creep resistance and better fatigue life could be achieved.

The production of MMCs is mainly achieved using two routes; either casting techniques, such as stir casting, or powder metallurgy techniques, such as mechanical alloying. Each of these processes has certain advantages and limitations. One main challenge in mechanical alloying is the difficulty to keep clean surfaces assuring coherent contact between the powders used [9]. Casting, as a liquid phase process, is capable of producing as-cast lightweight bulk components of MMCs. However, liquid phase casting processes usually results in poor properties obviously due to the defects arising from high melting temperatures at which the reinforcement is usually added. It is difficult to obtain uniform dispersion of the ceramic particles in liquid metals due to high viscosity, poor wettability in the metal matrix, and a large surface-to-volume ratio. These problems induce agglomeration and clustering [10].

The rheocasting (compocasting), as a semi-solid phase process, can produce good quality MMCs [6,11]. The technique has several advantages: It can be performed at temperatures lower than those conventionally employed in foundry practice during pouring; resulting in reduced thermochemical degradation of the reinforced surface, the material exhibits thixotropic behaviour typical of stir-cast alloys, and production can be carried out using conventional foundry methods. The preparation procedure for rheocast composites consists of the incorporation of the ceramic particles within very vigorously agitated semi-solid alloy slurry which can achieve more homogenous particles distribution as compared with a

fully molten alloy. This is because of the presence of the solid phase in the viscous slurry that prevents the ceramic particles from settling and agglomerating. However, the composites produced by rheocasting suffer from the high porosity content, which has a deleterious effect on the mechanical properties [11]. It has been reported that the porosity can be reduced by means of mechanical working such as extrusion or rolling on the solidified composites or by applying a pressure to the composite slurry during solidification [12-14].

However the mechanical characteristics of Al-based MMCs reinforced with microsize ceramic particulates at elevated temperatures was extensively studied [15-20], only limited data on the elevated temperatures bebaviour of Al-based nanocomposites are available. Until now the elevated temperatures mechanical properties for such nanocomposites were not sufficiently determined and published. This lack of data is more important when it is considered that elevated temperatures are often found in industrial applications, where the Al-based nanocomposites are being considered as candidates to replace steel or aluminum alloys. Typical examples are piston liners and cylindrical heads of automobile engines, as well as brake rotors.

The aim of the present investigation is to study the tensile behavior of A356/Al_2O_3 nanocomposites at both room and elevated temperatures up to 300˚C. The nanocomposites were fabricated using a combination of rheocasting and squeeze casting techniques. The effect of nanoparticles size and volume fractions on the tensile properties of the nanocomposites was investigated.

2. Experimental Procedures

The A356 Al-Si-Mg cast alloy was used as a matrix. The chemical composition of the A356 Al alloy is listed in **Table 1**. Nano-Al_2O_3 particulates have two different average sizes, typically, 200 and 60 nm were used as reinforcements. Several A356/Al_2O_3 nanocomposites containing different volume factions of Al_2O_3 nano-particulates up to 5 vol%.

The A356/Al_2O_3 nanocomposites were fabricated using a combination of rheocasting and squeeze casting techniques. Fabrication of the composite alloy was carried out according to the following procedures: About 1 kg of the A356 Al alloy was melted at 680˚C in a graphite crucible in an electrical resistance furnace. After complete melting and degassing by argon gas, the alloy was allowed to cool to the semisolid temperature of 602˚C. At such temperature the liquid/solid fraction was about 0.7. The liquid/solid ratio was determined using primarily differential scanning calorimeter (DSC) experiments performed on the A356 alloy. A simple mechanical stirrer with three blades made from stainless steel coated with bentonite clay (see **Figure 1**) was introduced into the melt and stirring was started at approximately 1000 rpm. The Al_2O_3 nano-particles were heated at 400˚C for two hours before dispersion inside the vortex formed due to stirring. After that, preheated Al_2O_3 nanoparticles were introduced into the matrix during the agitation. After completing the addition of Al_2O_3 nanoparticles, the agitation was stopped and the molten mixture was poured into preheated low carbon steel mould and immediately squeezed during solidification. T **Figure 2** shows a photograph of the mould used for squeezing the nanocomposites and the ingot after squeezing.

Samples from the cast nanocomposite ingots were cut from the cast ingot for microstructural examinations. Specimens were ground under water on a rotating disc using silicon carbide abrasive discs of increasing finesse

Table 1. The chemical composition (wt%) of the A356 alloy.

Si	Fe	Cu	Mn	Mg	Zn	Al
6.6	0.25	0.11	0.002	0.14	0.026	Bal.

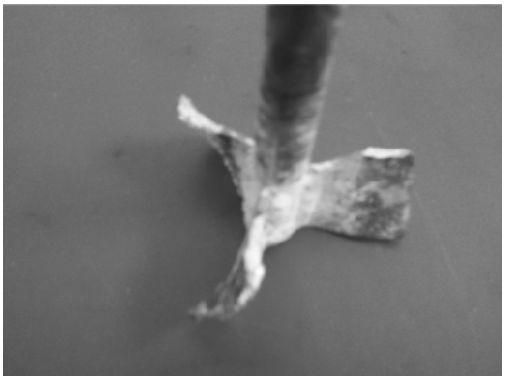

Figure 1. The three blades stirrer.

(a) (b)

Figure 2. The mould used to squeeze the nanocomposites (a) and the ingot after squeezing (b).

Samples from the cast nanocomposite ingots were cut from the cast ingot for microstructural examinations. Specimens were ground under water on a rotating disc using silicon carbide abrasive discs of increasing finesse up to 1200 grit. Then they were polished using 10 μm alumina paste and 3 μm diamond paste. Microstructural examinations were conducted using both optical and scanning electron microscopes (SEM). Microstructural examination was performed in the unetched condition. The porosity of the nanocomposites was measured using the typical Archimedes (water displacement) method.

The nanocomposites were heat treated at T6 before hardness and tensile testing. The nanocomposites were solution treated at 540 ± 1˚C for three hours and then quenched in cold water. After cooling specimens were artificially aged at 160 ± 1˚C for 12 hours. Microhardness was measured on polished samples using the Zwick/Roll microhardness tester. The tests were carried out by applying an indentation load of 25 g with a Vickers indenter. Minimum of ten readings were conducted for each specimen and the average value were considered. Tensile tests were carried out on composites after heat treatment at T6. Tensile tests were carried out at ambient, 100, 150, 200, 250 and 300˚C. The standard specimen used is shown in **Figure 3**. The specimens were machined longitudinally from the nanocomposite cast ingots. The tensile tests were carried out using 200 kN Shimadzu universal testing machine and a gripping device for non-threaded-end specimen according to ASTME 8-094. For each condition, minimum three specimens were tested and the average value was calculated.

The elevated temperatures tensile tests were conducted using electrical furnace. To insure that the temperature inside the furnace is stable, the specimen was heated to the test temperature for 30 min before each experiment. The temperature inside the furnace has an accuracy of ±5˚C. The cross head speed used in all tensile tests was 1 mm/min. The ultimate tensile strength (UTS), 0.2% yield stress (YS) and ductility (%E) measured by the elongation % were calculated.

3. Results and Discussion

3.1. Microstructural Observations

Figure 4 shows example micrographs of the microstructure of the monolithic A356 alloy as well as the A356/Al_2O_3 nanocomposites after heat treatment. It is clear from **Figure 4(a)** that the structure of the monolithic A356 Al alloy consists of primary α phase (white regions) and Al-Si eutectic structure (darker regions). Needle-like primary Si particulates were distributed along the boundaries of the α-Al dendrites. **Figures 4(b)** and **4(c)** show micrographs of nanocomposites containing 3 vol% of Al_2O_3 nanoparticulates having 60 and 200 nm, respecttively. Clusters of nanoparticles in the microstructure of the A356/Al_2O_3 nanocomposite were observed. The nanocomposites containing 5 vol% exhibited the highest agglomeration percent when compared with those containing 1 and 3 vol% (see **Figure 4(d)**). **Figure 4(e)** shows high magnification micrograph of Al_2O_3/5 vol% (200 nm) nanocomposites. It is clear that clusters of nanoparticles clusters are located inside the α-grains as well as near the eutectic structure. **Figure 5(a)** shows high magnification SEM micrograph of the 5 vol% Al_2O_3 nanoparticulates (200 nm) showing that nanoparticulates are agglomerating near the Si particles of the eutectic structure. The XRD analysis for the nanoparticles is shown in **Figure 5(b)** indicates the presence of Al_2O_3 nanoparticulates near the eutectic structure. Also, it has been observed that increasing the volume fraction of the nanoparticlutes dispersed inside the A356 alloy increases the agglomeration percent.

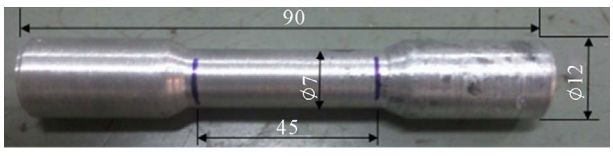

Figure 3. The tensile specimen (dimensions in mm).

Porosity measurements indicted that the nanocomposites have porosity content lower than 2 vol%. Such low porosity content is attributed to the squeezing process carried out during the solidification of the nanocomposites. Generally in cast MMCs, there are several sources of gases. The occurrence of porosity can be attributed variously to the amount of hydrogen gas present in the melt, the oxide film on the surface of the melt that can be drawn into it at any stage of stirring, and the gas being drawn into the melt by certain stirring methods [6,11]. Vigorously stirred melt or vortex tends to entrap gas and draw it into the melt. Increasing the stirring time allows more gases to be entered into the melt and hence reduce the mechanical properties.

The amount of liquid inside the semi-solid slurry increases with increasing the temperature which on the other hand reduces the viscosity of the solid/ liquid slurry. Nanoparticle distribution in the A356 Al matrix alloy during the squeezing process depends greatly on the viscosity of the slurry and also on the characteristics of the reinforcement particles themselves, which influence the effectiveness of squeezing in to break up agglomerates and distribute particles. When the amount of liquid inside the slurry is large enough, the particles can be rolled or slid over each other and thus breaking up agglomerations and helping the redistribution of nanoparticles and im-

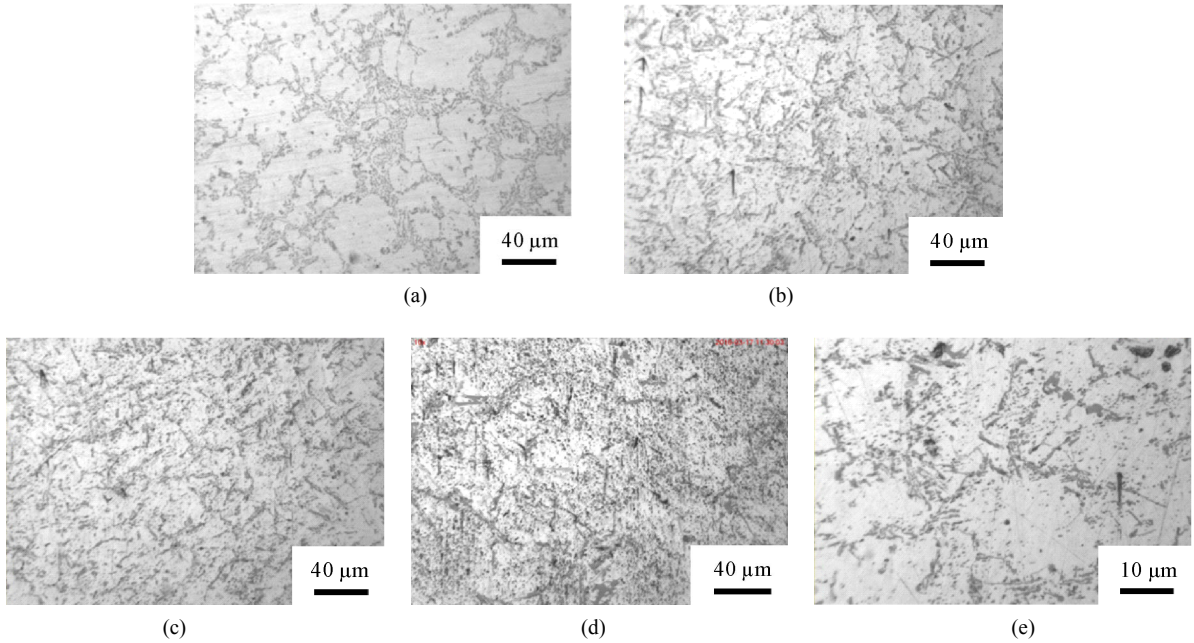

Figure 4. Optical micrographs for (a) A356 monolithic aluminum alloy; (b) A356/3 vol% Al_2O_3 (60 nm) nanocomposites; (c) A356/3 vol% Al_2O_3 (200 nm) nanocomposites; (d) A356/5 vol% Al_2O_3 (200 nm) (e) A356/5 vol% Al_2O_3 (200 nm) nanocomposites.

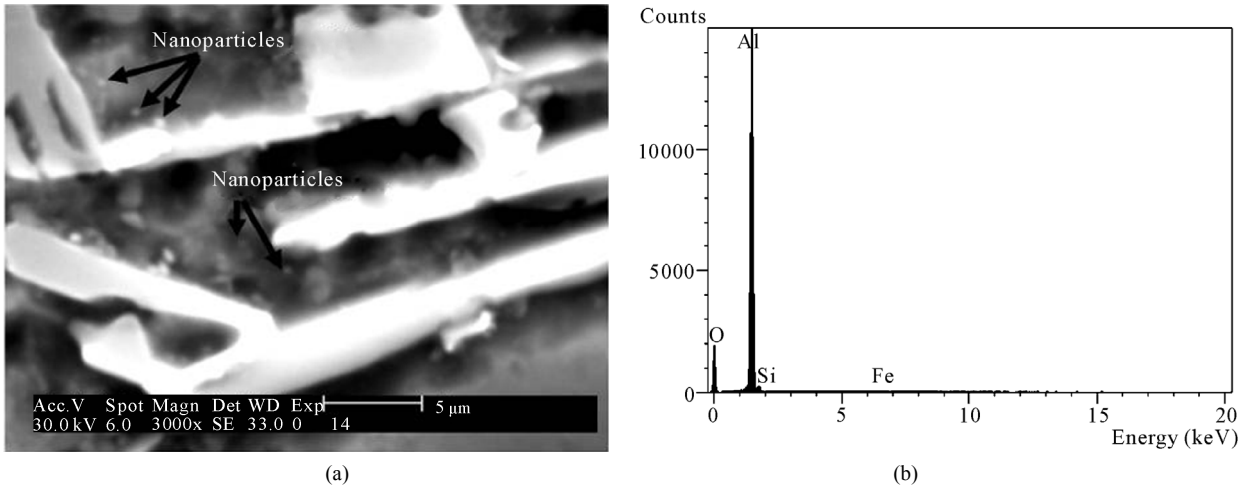

Figure 5. (a) High magnification SEM micrograph of the 5 vol% Al_2O_3 nanoparticulates (200 nm) showing that nanoparticulates are agglomerating near the Si particles of the eutectic structure; (b) XRD analysis for the particles shown in (a).

proving the microstructure.

3.2. Hardness of Nanocomposites

Figure 6 shows the variation of the microhardness of the nanocomposites with the volume fraction of Al_2O_3 nanoparticulates. It has been found that the nanocomposites exhibited higher average microhardness than the A356 monolithic alloy. The average microhardness of the nanocomposites increases with increasing the volume fraction of the Al_2O_3 nanoparticulates. The nanocomposites containing 200 nm Al_2O_3 nanoparticulates exhibited slightly higher average microhardness when compared with the nanocomposites containing 60 nm Al_2O_3 nanoparticulates. The increase of the hardness of the A356 alloy due to the addition of Al_2O_3 nanoparticulates may attribute to the increase of the resistance to localized plastic deformation.

The increase of the hardness due to the addition of ceramic nanoparticulates to aluminum and magnesium alloys were reported by many workers [7,8,21]. For exam-

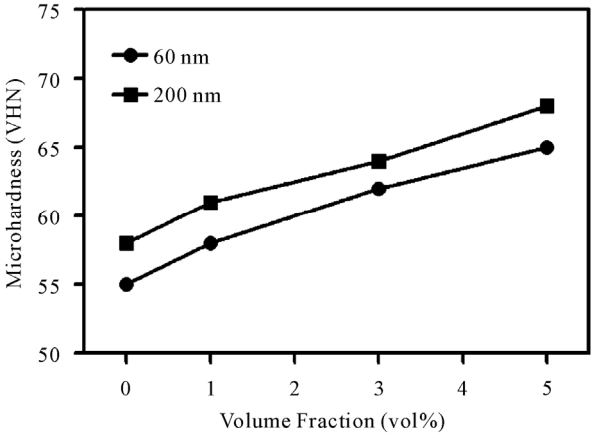

Figure 6. Variation of the microhardness of the nanocomposites with the volume fraction of Al_2O_3 nanoparticulates.

ple, *Ansary et al.* [21] studied the mechanical properties of A356.1 Al alloy reinforced with nano-sized MgO (50 nm) up to 5 vol%. The A356.1/MgO nanocomposites were fabricated via stir casting method. The results showed that the hardness of all composites is higher than A356.1 monolithic alloy due to the presence of MgO nanoparticulates with high hardness. The nanocomposites with 5 vol% content of MgO exhibited lower hardness than samples with 2.5 vol% MgO due to the presence of more porosity with the higher content of MgO.

3.3. Tensile Properties at Room Temperature

Figure 7 shows the variation of the tensile properties of the nanocomposites as well as the A356 unreinfrced matrix at room temperature. The tensile tests results reveled that both ultimate tensile and yield strengths of the nanocomposites are greater than the A356 monolithic alloy. For example, the A356 monolithic alloy exhibited average UTS and YS of about 221 and 181 MPa, respecttively. While the nanocomposites containing 5 vol% of 60 nm Al_2O_3 nanoparticles showed the maximum UTS and YS of about 282 and 245 MPa, respectively. This shows an increase of the UTS and YS by about 27% and 35%, respectively. The A356/Al_2O_3 nanocomposites exhibited higher ductility when compared with the A356 monolithic alloy. For example, the A356 monolithic alloy exhibited average % elongation of about 4% while the nanocomposites containing 5 vol% of 60 nm Al_2O_3 nanoparticles showed average % elongation of about 8%. This shows an increase of the elongation percent by about 50%. The nanocomposites reinforced with smaller Al_2O_3 nanoparticles size (*i.e.* 60 nm) exhibited higher UTS and YS when compared with the nanocomposites having larger Al_2O_3 nanoparticles size (*i.e.* 200 nm). Increasing the volume fraction of Al_2O_3 nanoparticles from

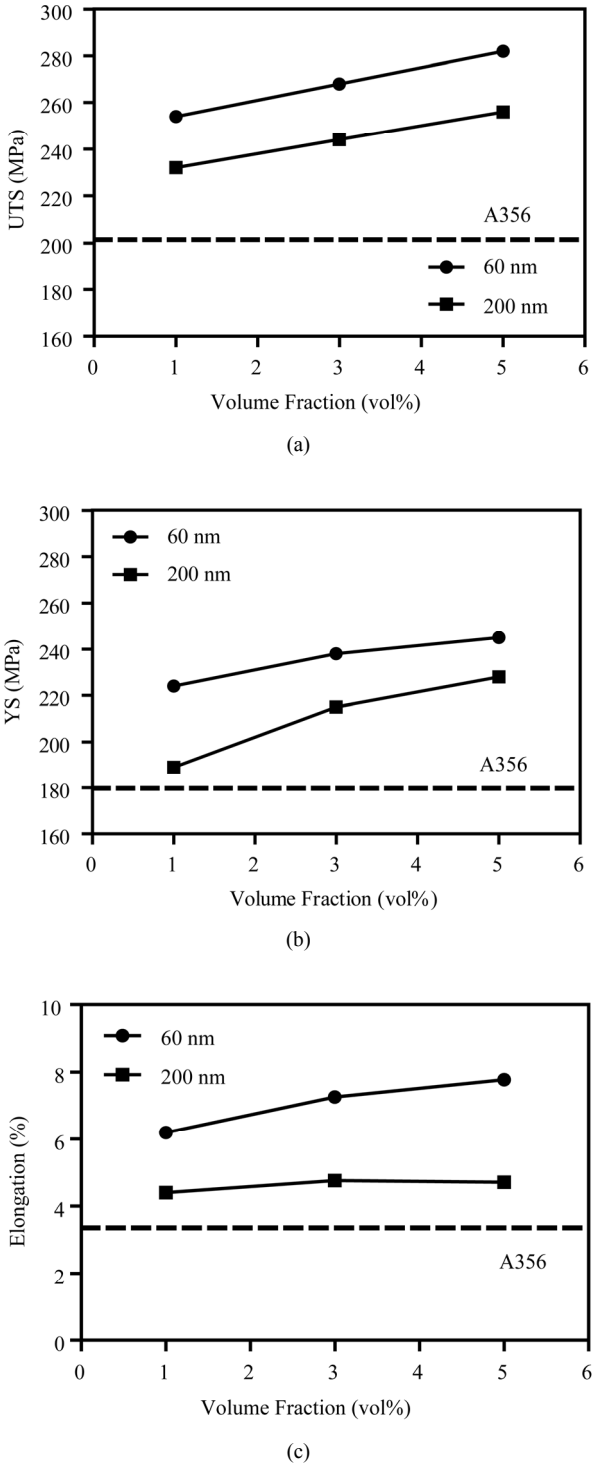

Figure 7. Tensile properties of A356/Al_2O_3 nanocomposites at room temperature; (a) ultimate tensile strength (UTS), (b) 0.2% yield strength (YS) and (c) elongation %.

1% to 5% increased considerably both the UTS and YS. While, increasing the volume fraction of Al_2O_3 nanopar-

ticles slightly increased the ductility of the nanocomposites.

The improvement of the tensile properties of the cast aluminum alloys due to the addition of nanoparticulates was reported by many workers [6,22]. For instance, El-Mahallawi *et al.* [6] studied the processing of A356 Al-Si alloy containing up to 5% vol% nanosize Al_2O_3 particles having size less than 500 nm. Nanocomposites were prepared using rheocasting (semi-solid) casting route. The results showed that introducing nano-particles into semi-solid slurries promises to be a successful route for producing a new generation of cast metal matrix nanocomposites. The nanocomposites showed high strength values associated with superior ductility compared to the alloy without particles addition under the same casting conditions. Young *et al.* [22] studied the tensile behavior of A356 Al alloy reinforced with nanosize Al_2O_3 particulates (30 nm). Nanocomposites containing up to 2 wt% of Al_2O_3 nanoparticulates were fabricated using ultrasonic processing at 760˚C. The results showed that with only 2 wt% nanosize SiC, the yield strength of as-cast Al alloy A356 was improved approximately 50%, which is significantly better than what Al alloy with the same percentage of micro-particle reinforcement can offer. They also noted that there is little change in the elongation and ultimate tensile strength.

The improved strength and ductility exhibited by the nanocomposites fabricated by the combination of rheocasting and squeeze casting technique may be attributed to: 1) The high effective viscosity of the molten slurry that prevents particles from settling, floating, or agglomerating during the stirring process; 2) The application of squeezing pressure during solidification which reduces greatly the porosity that may developed from the rheocasting step. These reasons lead to better distribution of the ceramic phase, reduction of porosity and hence better mechanical properties.

The strengthening mechanism for the metal matrix nanocomposites may attributed to the higher dislocation density in nanocomposites due to the addition of nanoceramic phase [22,23]. The difference of the coefficients of thermal expansion between the aluminum matrix and the uniformly dispersed nano-Al_2O_3 could develop high dislocation density, and the Al_2O_3 naoparticulates can work as the barriers for dislocations movement. It has been shown that the properties of nanocomposites would be enhanced considerably even with a very low volume fraction due to the high dislocation density of matrix metal.

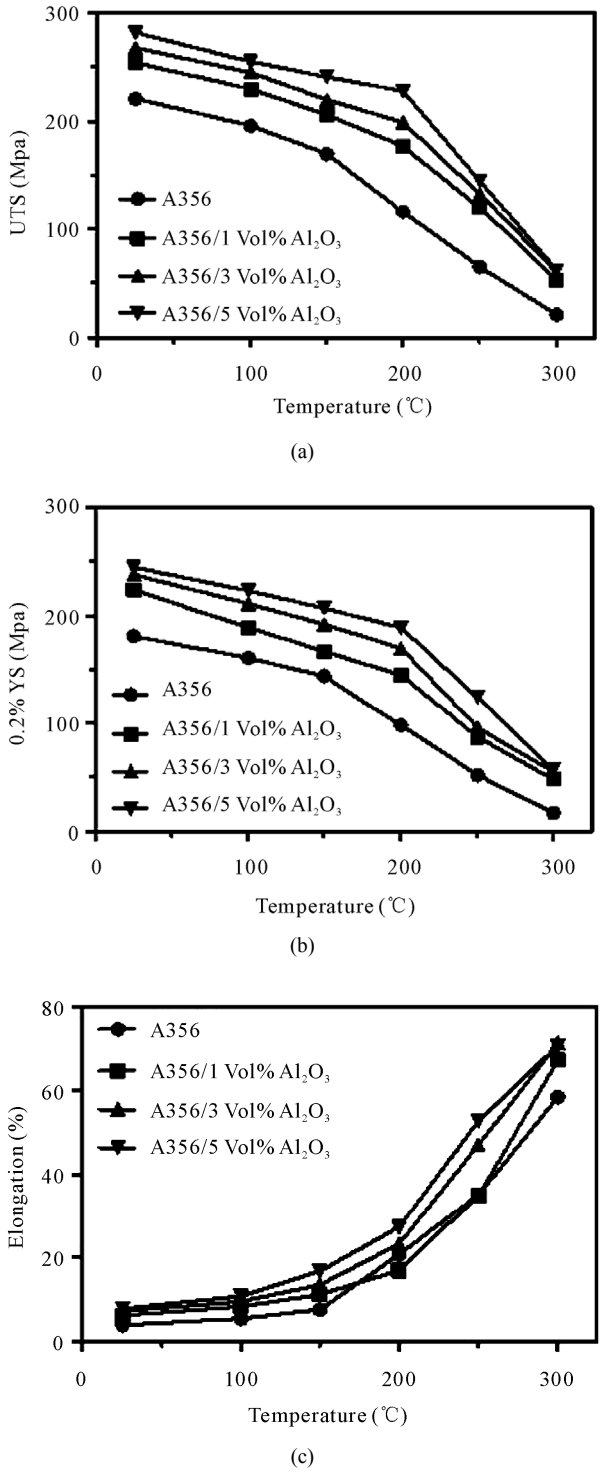

Figure 8. Variation of the A356/Al_2O_3 (60 nm) nanocomposites with temperature (a) ultimate tensile strength (UTS), (b) 0.2% yield strength (0.2% YS) and (c) the elongation %.

3.4. Tensile Properties at Elevated Temperatures

Figure 8 and **Figure 9** show the variation of the tensile properties with temperature for the nanocomposites containing 60 and 200 nm Al_2O_3 nanoparticulates, respec-

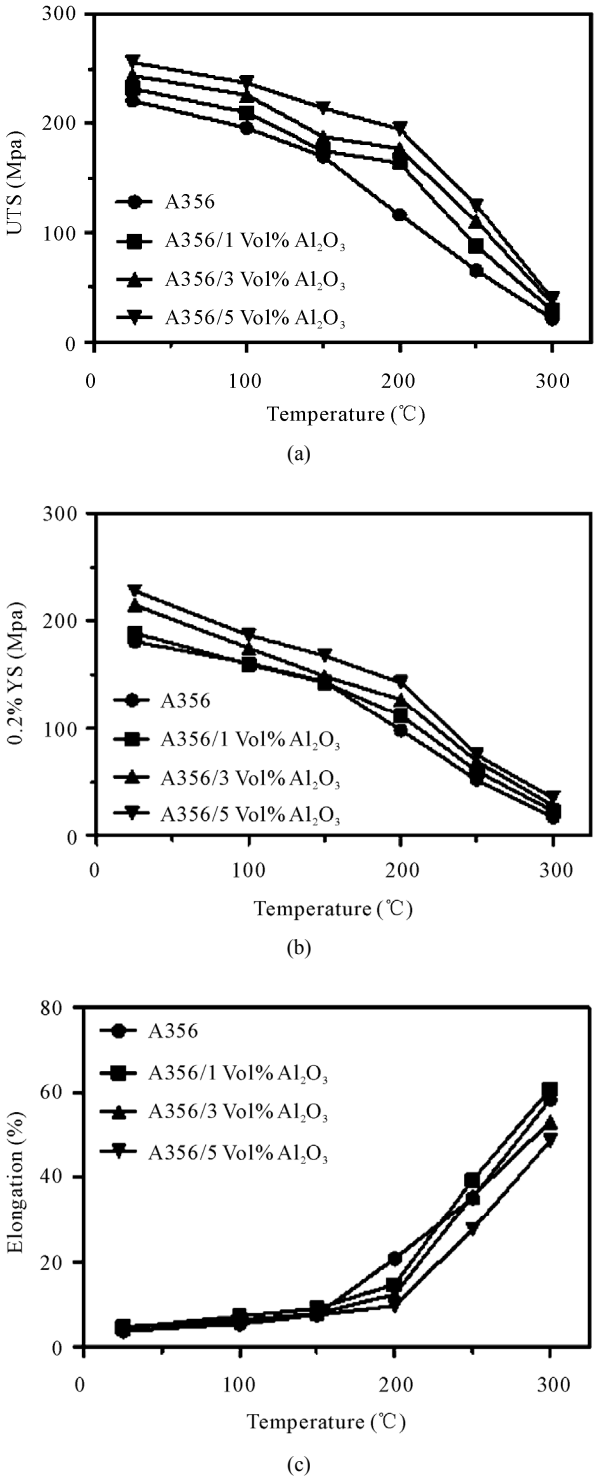

Figure 9. Variation of the A356/Al_2O_3 (200 nm) nanocomposites with temperature (a) ultimate tensile strength (UTS), (b) 0.2% yield strength (0.2% YS) and (c) the elongation %.

tively. The results showed that the nanocomposites exhibited better elevated temperature mechanical properties than the A356 unreinforced alloy. The UTS, 0.2% YS and ductility of the nanocomposites up to 300˚C are still higher than that of A356 monolithic alloy. For example, at 150˚C, the UTS of A356 monolithic alloy was 170 MPa while the UTS of A356/5 vol% Al_2O_3 (60 nm) nanocomposites was 241 MPa. Again, it has been found that reducing the size of the nanoparticulates from 200 nm to 60 nm and/or increasing the volume fraction of the nanoparticles from 1% to 5%, increase the tensile properties of the nanocomposite at elevated temperatures.

A sharp decrease of the tensile properties of the A356 monolithic alloy was observed after 150˚C. The temperature of about 150˚C was a critical temperature for the tensile properties of the A356 monolithic alloy. The nanocomposites exhibited a critical temperature of about 200˚C. Such observation was noticed for both alloys containing Al_2O_3 nanoparticulates of size of 60 and 200 nm. It can be concluded that at temperature higher than 200˚C, the matrix becomes soft, then the particles flow with the matrix, left voids, and hence reduce the strength.

The manner by which the reinforcing Al_2O_3 nanoparticulates affect the tensile strength of the aluminum alloy composite can be described in terms of work hardening. Beyond macroscopic yield a power law is representative of the stress versus strain curve. It is expressed by the Equation (1):

$$\sigma = K\left(\varepsilon_p\right)^n \tag{1}$$

where: K is the monotonic strength coefficient (intercept at plastic strain $\varepsilon_p = 1$) and 'n' is the work hardening or strain hardening exponent. In the A356/Al_2O_3 nanocomposites, with a large coefficient of thermal expansion (CTE) mismatch strain between the aluminum alloy metal matrix and the reinforcing nano-Al_2O_3 particulates, the plastic deformation of the ductile aluminum alloy metal matrix, in the presence of the discontinuous nano-Al_2O_3 reinforcements, is essentially nonuniform, *i.e.* heterogeneous. This is because of the hard, brittle and elastically deforming particles resisting plastic flow of the soft, ductile and plastically deforming aluminum alloy metal matrix. The plastic deformation induced dislocations, or slip dislocations, become dominant when the plastic strain exceeds the thermal mismatch strain and the two effects eventually act in synergism so that they can be lumped together.

The increased yield strength ($\Delta\sigma_y$) of the matrix of the Al_2O_3 nanoparticles reinforced A356 aluminum nanocomposites, due to dislocation generation and accumulation, and assuming the dislocations to be uniformly dispersed in the metal matrix, can be estimated using the Equation (2) [24]:

$$\Delta\sigma_v = \alpha G b (\rho)^{1/2} \quad (2)$$

where $\Delta\sigma_y$ is the increase in yield strength of the metal matrix composite over that of the unreinforced matrix alloy (aluminum alloy A356), G is the shear modulus (GPa) of the metal matrix, b is the Burgers vector, ρ is the increase in dislocation density of the composite matrix over that of the unreinforced matrix density, and α is a constant and is equal to 1.25 for aluminum.

The increase in flow stress of the discontinuously reinforced aluminum metal matrix composites over the unreinforced matrix alloy is proportional to the CTE mismatch strain if the dislocations generated by CTE mismatch strain are dominant. The mismatch strain (ε_α) induced in the particle is [25]:

$$\varepsilon_\alpha = (\alpha_p - \alpha_M)\Delta T \quad (3)$$

where: α_p and α_M are CTE of the ceramic particle (Al_2O_3) and the matrix (aluminum alloy A356) respectively, and both the matrix and the particle are assumed to be isotropic in stiffness and CTE. ΔT is the net temperature ($T_o - T_{ambient}$) change when the particulate-reinforced aluminum alloy metal matrix is quenched from an elevated temperature (say T_o).

Accordingly, the contributions to strengthening of the A356/Al_2O_3 nanocomposites can be arises from the mutually competitive influences of the following mechanisms: 1) Strengthening due to large differences in thermal coefficients of expansion between constituents of the composite, *i.e.* aluminum alloy and Al_2O_3, resulting in misfit strains due to differential thermal contraction at the Al/Al_2O_3 interfaces. The misfit strain and concomitant misfit stresses generate dislocations. The increased dislocation density generated to accommodate the misfit strains provides a positive contribution to strengthening the matrix of the nanocomposites; 2) Dispersion strengthening caused by the presence of reinforcing Al_2O_3 nanoparticles in the A356 aluminum alloy metal matrix and the additional stress required for slip dislocations to by-pass a reinforcing Al_2O_3 nanoparticles.

4. Conclusions

According the results obtained from the current investigation, the following conclusions can be pointed out:

1) The A356/Al_2O_3 nanocomposites exhibited better tensile properties than the A356 monolithic alloy. Such improvement in the tensile properties was observed at both room and elevated temperatures up to 300˚C. Increasing the volume fraction of the Al_2O_3 nanoparticulates increases both the tensile and yield strengths of the nanocomposites.

2) The nanocomposites having 60 nm Al_2O_3 nanoparticulates showed better room and elevated tensile properties than those containing 200 nm Al_2O_3 nanoparticulates.

3) The nanocomposites exhibited higher critical temperature, at which the tensile properties decrease sharply, than the A356 monolithic alloy. The nanocomposites and the A356 unreinforced alloy showed critical temperatures of 200˚C and 150˚C, respectively.

5. Acknowledgements

This work is supported by the King Abdel-Aziz City of Science and Technology (KACST) through the Science and Technology Center at King Khalid University (KKU), Fund (NAN 08-172-7). The authors thank both KACST and KKU for their financial support. Special Thanks to Prof. Dr. Saeed Saber, Vice President of KKU, Dr. Ahmed Taher, Dean of the Scientific Research at KKU, and Dr. Khaled Al-Zailaie**,** Dean of the faculty of engineering at KKU, for their support.

REFERENCES

[1] ASM Handbook, "Composites," *ASM International*, Vol. 21, 2001.

[2] N. Chawla and K. K. Chawla, "Metal Matrix Com- posites," Springer Science and Business Media Inc., New York, 2006,

[3] M. Kok, "Production and Mechanical Properties of Al_2O_3 Particle-Reinforced 2024 Aluminium Alloy Composites," *Journal of Materials Processing Technology*, Vol. 161, No. 3, 2005, pp. 381-387.

[4] T. S. Srivatsan, M. Al-Hajri, C. Smith and M. Petraroli, "The Tensile Response and Fracture Behavior of 2009 Aluminum Alloy Metal Matrix Composite," *Materials Science and Engineering*: *A*, Vol. 346, No. 1-2, 2003, pp. 91-100. doi:10.1016/S0921-5093(02)00481-1

[5] F. S. Rashed, M. R. Ibrahim and T. S. Mahmoud, "Microstructural and Mechanical Characteristics of A356/SiC_p MMCs Produced by Rheocasting Technique," *Journal of Engineering and Applied Sciences*, Vol. 52, No. 5, October 2005, pp. 1001-1018.

[6] I. S. El-Mahallawi, K. Eigenfield, F. Kouta, A. Hussein, T. S. Mahmoud, R. M. Ragaie, A. Y. Shash and W. Abou-Al-Hassan, "Synthesis and Characterization of New Cast A356/(Al_2O_3)P Metal Matrix Nano-Composites," *ASME*, *In the proceeding of the 2nd Multifunctional Nanocomposites & Nanomaterials*, *International Conference & Exhibition*, Cario, January 2008.

[7] J. Lan, Y. Yang and X. C. Li, "Microstructure and Microhardness of SiC Nanoparticles Reinforced Magnesium Composites Fabricated by Ultrasonic Method," *Materials Science and Engineering*: *A*, Vol. 386, No. 1-2, 2004, pp. 284-290.

[8] M. Habibnejad-Korayem, R. Mahmudi and W. J. Poole, "Enhanced Properties of Mg-Based Nano-Composites

Reinforced with Al_2O_3 Nano-Particles," *Materials Science and Engineering*: *A*, Vol. 519, No. 1-2, 2009, pp. 198-203. doi:10.1016/j.msea.2009.05.001

[9] F. Y. C. Boey, Z. Yuan and K. A. Khor, "Mechanical Alloying for the Effective Dispersion of Sub-Micron SiC_p Reinforcements in Al-Li Alloy Composite," *Materials Science and Engineering*: *A*, Vol. 252, No. 2, 1998, pp. 276-287. doi:10.1016/S0921-5093(98)00566-8

[10] J. Hashim, L. Looney and M. S. J. Hashmi, "Metal Matrix Composites: Production by the Stir Casting Method," *Journal of Materials Processing Technology*, Vol. 92-93, 1999, pp. 1-7. doi:10.1016/S0924-0136(99)00118-1

[11] T. S. Mahmoud, "Tribological Characteristics of A390/Gr_p MMCs Fabricated Using a Combination of Rheocasting and Squeeze Casting Techniques," *Proceedings of the IMechE, Part C*: *Journal of Mech. Engineering Science*, Vol. 222(C2), 2008, pp. 257-266.

[12] F. R. Rahmani and F. Akhlaghi, "Effect of Extrusion Temperature on the Microstructure and Porosity of A356-SiC_p Composites," *Journal of Materials Processing Technology*, Vol. 187-188, 2007, pp. 433-436. doi:10.1016/j.jmatprotec.2006.11.077

[13] P. Cavaliere, E. Cerri and E. Evangelista, "Isothermal Forging Modelling of 2618/20% Al_2O_{3p} Metal Matrix Composite," *Journal of Alloys and Compounds*, Vol. 378, No. 1-2, 2004, pp. 117-122. doi:10.1016/j.jallcom.2003.10.103

[14] J. Hashim, L. Looney and M. S. J. Hashmi, "Particle Distribution in Cast Metal Matrix Composites: Part I," *Journal of Materials Processing Technology*, Vol. 123, No. 2, 2002, pp. 251-257. doi:10.1016/S0924-0136(02)00098-5

[15] E. Y. EL-Kady, "Behavior of as Cast and Hot Rolled Composites at Room and Elevated Temperature," *Alexandria Engineering Journal*, Vol. 42, No. 6, 2003, pp. 669-680.

[16] T. A. Khalifa and T. S. Mahmoud, "Elevated Temperatures Mechanical Properties of Al Alloy AA6063/SiC_p MMCs," *Proceedings of World Congress on Engineering* 2009 (*WCE* 2009), London, Vol. II, July 2009, pp. 1557-1562.

[17] T. G. Nieh, D. R. Lesuer and C. K. Syn, "Tensile and Fatigue Properties of a 25 vol% SiC Particulate Reinforced 6090 Al Composite at 300˚C," *Scripta Metallurgica et Materialia*, Vol. 32, No. 5, 1995, pp. 707-712. doi:10.1016/0956-716X(95)91590-L

[18] J. W. Luster, M. Thumann and R. Baumann, "Mechanical Properties of Aluminum Alloy 6061-Al_2O_3 Composites," *Materials Science and Technology*, Vol. 9, 1993, pp. 853-862.

[19] J. Singh, S. K. Goel, and V. N. S. Mathur, "Elevated Temperature Tensile Properties of Squeezed-Cast Al-Al_2O_3-MgO Particulate MMCs up to 573 K," *Journal of Materials Science*, Vol. 26, No. 10, 1991, pp. 2750-2758. doi:10.1007/BF02387746

[20] J. Oñoro, M. D. Salvador and L. E. G. Cambronero, "High-Temperature Mechanical Properties of Aluminium Alloys Reinforced with Boron Carbide Particles," *Materials Science and Engineering*: *A*, Vol. 499, No. 1-2, 2009, pp. 421-426. doi:10.1016/j.msea.2008.09.013

[21] A. A. Yar, M. Montazerian, H. Abdizadeh and H. R. Baharvandi, "Microstructure and Mechanical Properties of Aluminum Alloy Matrix Composite Reinforced with Nano-Particle Mgo," *Journal of Alloys and Compounds*, Vol. 484, No. 1-2, 2009, pp. 400-404. doi:10.1016/j.jallcom.2009.04.117

[22] Y. Yang, J. Lan and X. C. Li, "Study on Bulk Aluminum Matrix Nano-Composite Fabricated by Ultrasonic Dispersion of Nano-Sized SiC Particles in Molten Aluminum Alloy," *Materials Science and Engineering*: *A*, Vol. 380, No. 1-2, 2004, pp. 378-383. doi:10.1016/j.msea.2004.03.073

[23] B. H. Tian, P. Liu, K. X. Song, Y. Li, Y. Liu, F. Z. Ren and J. H. Su, "Microstructure and Properties at Elevated Temperature of a Nano-Al_2O_3 Particles Dispersion-Strengthened Copper Base Composite," *Materials Science and Engineering*: *A*, Vol. 435-436, 2006, pp. 705-710. doi:10.1016/j.msea.2006.07.129

[24] R. J. Arsenault, In: R. K. Everett and R. J. Arsenasult Eds., "Metal Matrix Composites: Mechanisms and Properties," Academic Press, San Diego, 1991, pp. 79-87.

[25] R. U. Vaidy and K. K. Chawla, "Thermal Expansion of Metal Matrix Composites," *Composites Science and Technology*, Vol. 50, No. 1, 1994, pp. 13-22 doi:10.1016/0266-3538(94)90122-8.

